Int. J. Solids Structures Vol. 20, No. 5, pp. 499–511, 1984
Printed in Great Britain.

0020-7683/84 $3.00 + .00

RESPONSE OF POROELASTIC LAYERS TO MOVING LOADS

MICHAEL BURKE
David W. Taylor Naval Ship R&D Center, Bethesda, MD 20084, U.S.A.

and

HERBERT B. KINGSBURY
Department of Mechanical and Aerospace Engineering, University of Delaware, Newark, DE 19711, U.S.A.

(*Received* 10 *February* 1983; *in revised form* 25 *July* 1983)

Abstract—This paper presents a study of the response of layers of fluid-filled porous elastic (poroelastic) materials to surface tractions moving at constant speed.

Solutions are obtained to Biot's equations for poroelastic materials using a Fourier Transform Method. Although physical domain behavior is found using a Fast Fourier transform for numerical inversion, it is shown that the distribution of fluid flow, pressure, stress and displacement may be determined directly in the transform domain without recourse to inversion.

Layer response to a moving porous indenter and to a moving fluid pressure wave is determined. The flow, pressure and stress distributions for the two cases are found to be markedly different.

INTRODUCTION

The response of fluid-filled porous elastic—or poroelastic—materials to load is a subject of importance in a number of fields. One particular class of poroelastic problems, that of a moving surface traction acting on a poroelastic layer or half-space, occurs in such disparate technologies as ocean engineering, soil mechanics, tribology, biomechanics and paper manufacturing.

Mukhopadhyay and Kingsbury[1] studied the flow and deformation in a layered poroelastic system subjected to a moving Gaussian shaped surface traction which was continuously distributed over both the solid and fluid phases of the material system. They found a speed dependent asymmetric distribution of flow through the surface, with fluid imbibition in front of the moving load and exudation behind. Lai and Mow[2] considered a poroelastic layer composed of incompressible constituents loaded by a moving porous indenter. The surface traction for this case was parabolic in shape and finite in extent. The moving load was carried by the solid phase only while the fluid phase could flow freely through the indenter. Their results also show an asymmetric surface flow but one with exudation in front of the moving load and imbibition behind. Yamamoto *et al.*[3], applied a traveling sinusoidal pressure wave to the surface of a poroelastic half-space with compressible constituents and determined a material property dependent phase lag of the pressure field which increased with distance into the layer. The predicted pressure gradient implies a surface flow into the layer ahead of a wave crest and out of the layer behind.

The preceding results suggest that fluid flow and pressure as well as solid phase deformation are effected both in distribution as well as magnitude by poroelastic material properties or by representation of the moving surface traction. In the present analysis it is shown that poroelastic layers are capable of exhibiting both described types of behavior and that the different types of flow fields are associated primarily with the distribution of the surface traction between the two phases.

It is also shown that the distribution of flow, pressure and deformation can be predicted on the basis of the solutions of the governing equations in the Fourier transform domain so that recourse to numerical evaluation of the solutions is required only to demonstrate the details of the predicted solution.

GOVERNING EQUATIONS

Beginning in 1941, Biot published a series of papers[4–9] dealing with a general theory of behavior of what are now termed poroelastic materials. A less intuitive approach than Biot's has been adapted by a number of investigators including Adkins[10, 11], Green and

Adkins[12], Green and Naghdi[13], Bowen[14, 15], Rice and Cleary[16], and others. The Biot theory is a special case of these more complete formulations but, as has been pointed out by Rice and Cleary[16], the latter may present little or no improvement on the classical Biot formulation for quasi-static elastic deformation problems.

The quasistatic poroelastic theory as presented by Biot is based on several fundamental assumptions. The two-phase poroelastic material is considered to be composed of a solid framework possessing a statistical distribution of small pores which are filled with, in general, a Newtonian viscous, compressible fluid. The bulk material is assumed to be homogeneous on a microscopic scale and the pores to be all interconnected. The deformations of the solid and fluid are taken to be reversible with the solid skeleton being linearly elastic and undergoing small deformations. The fluid flow is assumed to follow Darcy's law of filtering. The fluid shear stresses are assumed to be small compared to the fluid pressure and the solid phase stresses. The inertia forces, considered in the dynamic theory, are also considered to be negligibly small.

The reference porosity, "f", of a poroelastic material is defined as the ratio of pore volume to the total volume of the undeformed material. In the subsequent analysis the actual porosity is assumed to be unchanged from the reference porosity. As discussed by Bear[17], the assumption of homogeneity implies that the porosity is also equal to the ratio of the void area to the total area of any cross section of the bulk material.

The average stress on the bulk material, τ_{ij}, which is called the total stress is related to the actual solid phase stress, σ_{ij}, and the fluid pressure, p, by the relationship:

$$\tau_{ij} = (1-f)\sigma_{ij} - fp\delta_{ij}. \tag{1}$$

It is convenient to introduce effective solid (S_{ij}) and fluid (σ) stresses through the following definition.

$$S_{ij} = (1-f)\sigma_{ij}, \quad \sigma = -fp. \tag{2}$$

Although it is possible to define a solid displacement field within the solid phase and a fluid displacement field within the fluid phase, the locations of the solid and fluid phase must then be monitored in order to know which displacement vector is defined at an arbitrary point within the material. To eliminate this ambiguity, solid displacements and fluid displacements, u_i, U_i, are introduced such that at each point within the material both an average solid displacement and an average fluid displacement are defined.

The deformation of the poroelastic material is expressed in terms of the average displacement fields in the usual manner, assuming strains and angles of rotation are small compared to unity. The components of strain for the solid, ϵ_{ij}, are defined as:

$$\epsilon_{ij} = \left(\frac{\partial u_i}{\partial X_j} + \frac{\partial u_j}{\partial X_i}\right). \tag{3}$$

Similarly, the solid dilatation, ϵ, and the fluid dilatation, e, are defined by:

$$\epsilon = \frac{\partial u_i}{\partial X_i}, \qquad e = \frac{\partial U_i}{\partial X_i}. \tag{4}$$

An additional measure of solid and fluid strain, ζ, may also be introduced. This quantity, defined as

$$\zeta = (e - \epsilon) \tag{5}$$

represents the increment of fluid content in the porous material during deformation.

It is seen that the state of strain in a poroelastic material may be described by six components of solid strain and the fluid dilatation, and the state of stress may be described by six components of solid stress and the fluid stress.

Four independent poroelastic coefficients are required to characterize a linear isotropic poroelastic material. The following form of stress–strain relations, introduced by Biot[6–8], and by Biot and Willis[18], is employed in the present formulation

$$S_{ij} = 2\mu\epsilon_{ij} + \delta_{ij}(\lambda\epsilon + \gamma e) \tag{6a}$$

$$\sigma = \gamma\epsilon + \beta e. \tag{6b}$$

The measurement and physical interpretation of the coefficients μ, λ, γ, and β is discussed by Biot and Willis[18], and by Kingsbury[19].

In the absence of body forces the total stress components satisfy the stress equilibrium equations:

$$\frac{\partial \tau_{ij}}{\partial X_i} = 0. \tag{7}$$

Equations analogous to the Navier equations of elasticity are obtained by combining the constitutive equations with the stress equilibrium equations in terms of the average fluid and solid phase stresses (1), (2), employing eqns (6) and (7), and assuming the material coefficients are not functions of the spatial coordinates, the following equations of equilibrium result.

$$\mu\frac{\partial^2 u_j}{\partial X_i \partial X_i} + (\lambda + \gamma + \mu)\frac{\partial \epsilon}{\partial X_j} + (\gamma + \beta)\frac{\partial e}{\partial X_j} = 0. \tag{8}$$

Formulation of the governing equations is completed by stating Darcy's Law of filtering in terms of the variables of the system. This equation may be written as[17, 20]:

$$\frac{\partial}{\partial t}(U_i - u_i) = \frac{K}{\eta f}\frac{\partial \sigma}{\partial X_i} \tag{9}$$

where K is the permeability and η is the dynamic viscosity of the fluid. The term, $(\partial/\partial t)(U_i - u_i)$, is the velocity of the fluid phase with respect to the solid phase, which is called the filtering velocity. As shown by Biot[9] the rate of energy dissipation per unit volume (D) is related to the filtering velocity components by the equation:

$$D = \frac{1}{2}\eta/K\sum_{i=1}^{3}\frac{\partial}{\partial t}(U_i - u_i)^2. \tag{10}$$

In the present analysis eqns (8) and (9) are recast in terms of the variable ζ and the solid phase displacement components in the following form:

$$\mu\nabla^2\tilde{u} + (\lambda + 2\gamma + \mu + \beta)\nabla\epsilon = -(\gamma + \beta)\nabla\zeta \tag{11}$$

$$K_{lfn}\left[\beta - \frac{(\gamma + \beta)^2}{(\lambda + 2\mu + 2\gamma + \beta)}\right]\nabla^2\zeta = \frac{\partial \zeta}{\partial t}. \tag{12}$$

Equation (12) indicates that ζ is dissipative in nature, so eqn (11) can be viewed as the classical elasticity formulation subjected to a dissipative body force.

If the variable ζ represented temperature, then eqns (10) and (11) would be a form of the uncoupled equations of thermoelasticity. The subsequent method of solution could therefore be applied to problems of thermoelasticity although the particular poroelasticity boundary value problems solved in this paper do not correspond to commonly encountered boundary value problems of thermoelasticity.

SOLUTION FOR THE MOVING LOAD PROBLEM

The general problem to be considered is the response of a poroelastic layer of thickness h to a surface traction moving with constant speed, V_L. The traction distribution which is assumed to be uniform in the Z direction (plane strain), may be a continuous or discontinuous function of x, and may act on both the fluid and solid phases or may act on the solid phase only. Explicit time dependence in the governing equations is eliminated by a coordinate transformation from a fixed (X_1, X_2) coordinate system to a system (x, y) which is moving to the left (negative X_1 direction) with the moving surface traction so that:

$$x = X_1 + V_L t$$

$$y = X_2.$$

The plain strain form of eqns (11) and (12) can then be phrased as:

$$\nabla^2 u + (1 + ND_1 + ND_2)\frac{\partial \epsilon}{\partial x} + (ND_2)\frac{\partial \zeta}{\partial x} = 0 \tag{13a}$$

$$\nabla^2 v + (1 + ND_1 + ND_2)\frac{\partial \epsilon}{\partial y} + (ND_2)\frac{\partial \zeta}{\partial y} = 0 \tag{13b}$$

$$\nabla^2 \zeta - \frac{ND_3}{\left[1 - \dfrac{\alpha/fND_2}{2 + ND_1 + ND_2}\right]}\frac{\partial \zeta}{\partial x} = 0 \tag{14}$$

where

$$ND_1 = \frac{\lambda + \gamma}{\mu}, \qquad ND_2 = \frac{\alpha\beta}{f\mu}$$

$$ND_3 = V_L h \frac{f\eta}{K\beta},$$

$$u = u_x/h, \qquad v = u_y/h$$

and the x and y coordinates have been non dimensionalized with respect to h so that the layer thickness is unity.

It may be shown[9, 18], that $f < \alpha \leq 1$ and that $\alpha = 1$ if the material comprising the solid phase is incompressible.

Solution of eqns (13) and (14) proceeds by taking the Fourier transform with respect to the "x" coordinate using the following Fourier transform pair:

$$\hat{h}(\omega) = \int_{-\infty}^{\infty} h(x)\, e^{-i\omega x}\, dx, \quad h(x) = \frac{1}{2\pi}\int_{-\infty}^{\infty} \hat{h}(\omega)\, e^{i\omega x}\, d\omega$$

where $h(x)$ represents any of the dependent variables.

The transformed equations may then be phrased in the following form:

$$\hat{u}'' + i\omega A\hat{v}' - \omega^2(1 + A)\hat{u} = -i\omega B\hat{\zeta} \tag{15a}$$

$$(1 + A)\hat{v}'' + i\omega A\hat{u}' - \omega^2\hat{v} = -B\hat{\zeta}' \tag{15b}$$

$$\hat{\zeta}'' - \bar{k}^2\hat{\zeta} = 0 \tag{16}$$

where

$$\tilde{k}^2 = \omega^2 + i\omega C, \qquad A = 1 + ND_1 + ND_2$$

$$B = ND_2 \qquad C = \frac{ND_3}{\left[1 - \dfrac{\alpha/f\ ND_2}{2 + ND_1 + ND_2}\right]}$$

and superscript "prime" indicates differentiation with respect to "y". The general solution to eqn (16) is:

$$\hat{\zeta} = C_1 \sinh(\tilde{k}y) + C_2 \cosh(\tilde{k}y). \tag{17}$$

Upon substitution of eqn (17) into eqn (15) the following solution to that pair of equations is determined:

$$\hat{u} = \left[(iB_1 - B_2) + \left(\frac{A+2}{A\omega}\right)(iB_3 + B_4) + (iB_3 - B_4)y\right]\sinh \omega y$$
$$+ \left[(iB_1 + B_2) + \left(\frac{A+2}{A\omega}\right)(iB_3 - B_4) + (iB_3 + B_4)y\right]\cosh \omega y$$
$$+ \frac{i\omega B}{(1+A)(\omega^2 - \tilde{k}^2)}[C_1 \sinh \tilde{k}y + C_2 \cosh \tilde{k}y] \tag{18a}$$

$$\hat{v} = [(B_1 - iB_2) + (B_3 - iB_4)y]\sinh \omega y + [(B_1 + iB_2) + (B_3 + iB_4)y]\cosh \omega y$$
$$+ \frac{B\tilde{k}}{(1+A)(\omega^2 - \tilde{k}^2)}[C_2 \sinh \tilde{k}y + C_1 \cosh \tilde{k}y]. \tag{18b}$$

The subscripted constants B_j ($j = 1 - 4$) and C_i ($i = 1, 2$) are to be determined by the boundary conditions.

Since the above solutions are singular at $\omega = 0$, solutions for that case are found separately. The governing equations with the parameter ω equal to zero become:

$$\hat{u}'' = 0 \tag{19a}$$

$$(1+A)\hat{v}'' = -B\hat{\zeta}' \tag{19b}$$

$$\hat{\zeta}'' = 0. \tag{20}$$

The general solution to these equations is:

$$\hat{u} = E_1 y + E_2 \tag{21a}$$

$$\hat{v} = \frac{-BD_1}{2(1+A)}y^2 + F_1 y + F_2 \tag{21b}$$

$$\hat{\zeta} = D_1 y + D_2. \tag{22}$$

Once again, the subscripted letters E, D, F, are constants to be determined by the boundary conditions. The solutions at $\omega = 0$ complete the general solution of the transformed equations and, as will be discussed, they also provide significant information by themselves.

The bottom ($y = 0$) of the layer is considered to be attached to a rigid, impermeable

foundation, so the boundary conditions are:

$$u(x,0)=0, \quad v(x,0)=0, \quad \frac{\partial\sigma}{\partial y}(x,0)=0. \tag{23}$$

It will be assumed that the moving load does not impose a shear traction on the surface of the layer. When phrased in terms of displacements this condition becomes:

$$\partial u/\partial y(x,1)+\partial v/\partial x(x,1)=0. \tag{24}$$

The action of the moving load on the surface may be prescribed in terms of solid phase normal displacement or normal stress and of the normal filtering velocity or pressure. One problem considered here is that of a moving pressure wave, $p_s(x)$, which is supported by both the fluid and the solid phases. This is represented by:

$$S_{yy}|_{y=1}=-(1-f)p_s(x), \quad \sigma|_{y=1}=-fp_s(x). \tag{25a}$$

The second problem is that of a moving porous indenter which imposes a surface stress on the solid phase but which allows the fluid to drain freely through the surface. This is represented by:

$$S_{yy}|_{y=1}=-p_s(x), \quad \sigma|_{y=1}=0. \tag{25b}$$

The solutions for the problems represented by each of these surface stress conditions are obtained by determining the constants of integration appearing in eqns (17), (18), (21), (22) after expressing the boundary conditions in terms of the transform variables.

These solutions may then be phrased in the following form:

$$\hat{u}=B_3H_{11}(y,\omega)+B_2H_{12}(y,\omega) \tag{26a}$$

$$\hat{v}=B_3H_{21}(y,\omega)+B_2H_{22}(y,\omega) \tag{26b}$$

$$\sigma=B_3H_{31}(y,\omega)+B_2H_{32}(y,\omega) \tag{26c}$$

$$\frac{\partial\hat{u}}{\partial y}=B_3G_{11}(y,\omega)+B_2G_{12}(y,\omega) \tag{26d}$$

$$\frac{\partial\hat{v}}{\partial y}=B_3G_{21}(y,\omega)+B_2G_{22}(y,\omega) \tag{26e}$$

$$\frac{\partial\hat{\sigma}}{\partial y}=B_3G_{31}(y,\omega)+B_2G_{32}(y,\omega). \tag{26f}$$

Where the functions $H_{ij}(y,\omega)$ and $G_{ij}(y,\omega)$ are common to both surface traction problems but constants B_2 and B_3 are different for the cases described by eqns (25a) and (25b). These functions and constants are presented in Appendix A.

It is easily shown[21] that the Nth moment of a function $h(x)$ about the point $x=0$ is given by:

$$\int_{-\infty}^{\infty}x^Nh(x)\,dx=(i)^N\frac{d^N\hat{h}}{d\omega^N}\bigg|_{\omega=0}. \tag{27}$$

Also, the distance to the centroid of $h(x)$ is:

$$h_{cen}=\frac{-d\hat{h}/d\omega|_{\omega=0}}{i\hat{h}(0)} \tag{28a}$$

and the variance "$\bar{\sigma}^2$" is given by:

$$\bar{\sigma}^2 = -\frac{\left.\frac{d^2\hat{h}}{d\omega^2}\right|_{\omega=0}}{\hat{h}(0)} + \frac{\left(\left.\frac{d\hat{h}}{d\omega}\right)_{\omega=0}\right)^2}{\hat{h}^2(0)}. \tag{28b}$$

From the above results it is seen that information concerning the patterns of surface flow, pressure distribution, and displacement can be obtained without inversion of these variables to the real domain.

The values of the desired functions in the transform domain at $\omega = 0$ are given by—or obtained from—eqns (21) and (22) with appropriately specified values of the constants of integration.

To obtain the values of the first derivities of these functions at $\omega = 0$, eqns (15) and (16) are differentiated with respect to ω and the transform variable then set equal to zero. This process yields the equations:

$$\left.\frac{d\hat{\zeta}''}{d\omega}\right|_{\omega=0} - iC\hat{\zeta}(0,y) = 0 \tag{29}$$

$$\left.\frac{d\hat{u}''}{d\omega}\right|_{\omega=0} + iA\hat{v}'(0,y) = -iB\hat{\zeta}(0,y) \tag{30a}$$

$$(1+A)\left.\frac{d\hat{v}''}{d\omega}\right|_{\omega=0} + iA\hat{u}'(0,y) = -B\frac{d\hat{\zeta}'}{d\omega}(0,y). \tag{30b}$$

Since $\hat{\zeta}(0,y)$, $\hat{u}(0,y)$ and $\hat{v}(0,y)$ have been obtained, eqns (29) and (30) may be integrated with respect to y and the resulting constants of integration evaluated employing the boundary conditions appropriate to either the moving pressure wave problem or the moving indenter problem. Once the first derivatives of the transformed variables with respect to ω have been evaluated at $\omega = 0$, the process may be repeated as necessary to obtain derivatives of any order.

RESULTS

Expressions for the moments of the displacement, flow and stress variables obtained by evaluating the transformed variables and their derivatives at $\omega = 0$ are next presented. The layer response indicated by these analytical solutions is then compared with results in graphical form obtained by numerically inverting the transform domain solutions using a discrete inverse Fourier transform algorithm.

Response of the poroelastic layer to the moving surface pressure wave (eqn 25a) is considered first. The average value of the "y" displacement and its first moment are given by:

$$\int_{-\infty}^{\infty} v(x,y)\,dx = \frac{-(1-\alpha)}{\alpha/fG}\,y\int_{-\infty}^{\infty} p_s(x)\,dx \tag{31a}$$

$$\int_{-\infty}^{\infty} xv(x,y)\,dx = \frac{ND_3}{G}\left[f - \frac{(1-\alpha)ND_2}{G}\right](y - y^3/3)\int_{-\infty}^{\infty} p_s(x)\,dx \tag{31b}$$

where

$$G \equiv 2 + ND_1 - (\alpha/f - 1)ND_2.$$

It may be shown that $G > 0$[22].

Equation (31a) shows that the average y component of the displacement varies linearly with y and that if the material comprising the solid phase in incompressible ($\alpha = 1$) its value

is zero. The moment is proportional to the load and, through (ND_3), to the speed of the moving wave. Since ND_3 is intrinsically positive and the bracketed term in eqn (31b) has been found to be positive for a variety of poroelastic materials[22], the sign of the moment is therefore positive which means the surface displacement has a greater positive value behind the wave.

The integral of the y component of the filtering velocity is equal to zero indicating there is no net fluid imbibation or exudation through the surface. By eqn (9) the first moment of this filtering velocity component is proportional to the first moment of $\partial\sigma/\partial y$ which is given by:

$$\int_{-\infty}^{\infty} x\partial\sigma/\partial y \, dx = +ND_3\left[f - \frac{(1-\alpha)ND_2}{G}\right] y \int_{-\infty}^{\infty} p_s(x)\, dx. \tag{32}$$

The sign of this term indicates fluid exudation occurs behind the pressure wave.

The centroid of the fluid stress, σ, is given by:

$$\sigma_{cen} = \frac{ND_3}{2f}\left[f - \frac{(1-\alpha)ND_2}{G}\right](1-y^2). \tag{33}$$

Since the position of the centroid shifts in the positive x direction as y decreases, the centroid of the fluid pressure increasingly lags behind the centroid of the applied load with distance from the surface. This shift, which increases with pressure wave speed and layer thickness, is consistent with the preceding observation concerning the flow pattern through the surface.

Results for the totally permeable indenter problem, where the entire load is carried by the solid phase, are next presented.

Although the average value of the fluid stress is zero for this case, the first moment of the fluid stress is given by:

$$\int_{-\infty}^{\infty} x\sigma \, dx = \frac{ND_3}{G}\frac{(1-y^2)}{2}\int_{-\infty}^{\infty} p_s(x)\, dx. \tag{34}$$

This result indicates increased pore pressure exists ahead of the load and a region of decreased pore pressure behind it.

The integral of the "y" component of the filtering velocity is also zero, while this first moment of this quantity:

$$\int_{-\infty}^{\infty} x\partial\sigma/\partial y \, dx = \frac{-ND_3}{G} y \int_{-\infty}^{\infty} p_s(x)\, dx \tag{35}$$

indicates that fluid exudation exists ahead of the load for this surface traction and imbibation occurs behind.

Finally the average value and the first moment of the "y" displacement component are given by:

$$\int_{-\infty}^{\infty} v(x,y)\, dx = \frac{-y}{\alpha/fG}\int_{-\infty}^{\infty} p_s(x)\, dx \tag{36a}$$

$$\int_{-\infty}^{\infty} xv(x,y)\, dx = \frac{-ND_2ND_3}{G^2}\frac{(y - y^3/3)}{2}\int_{-\infty}^{\infty} p_s(x)\, dx. \tag{36b}$$

The sign of this moment indicates a greater positive surface displacement in front of the pressure wave than behind it.

To illustrate the preceding results, the analytical solutions obtained in the transform domain were inverted numerically using an FFT algorithm. The surface traction employed

for both the moving pressure wave and the porous indenter problems, which is shown in Fig. 1, is given by:

$$p_s(x) = p_0/2\left[1 + \cos\left(\frac{\pi x}{2}\right)\right] - 2 < x < 2$$

where the amplitude is chosen to give a unit non-dimensional load. In the subsequent figures displacement, stress, and velocity are non-dimensionalized by multiplication by $1/h$, $\alpha/f\mu$, and $1/V_L$ respectively.

The material system considered is wool felt-water whose poroelastic properties as reported in [22] are presented in Appendix B.

The effects of surface traction speed and type on normal surface displacement are shown in Figs. 2 and 3. The maximum displacement is greater under the indenter because the surface load is not shared by the fluid. As predicted by eqns (31b) and (36b) the outward displacement is larger behind the pressure load and in front of the indenter.

The effects predicted in the $\omega = 0$ solution for the surface filtering velocity are illustrated in Figs. 4 and 5 which shows exudation ahead of the indenter and imbibation behind, while exudation is greater behind the pressure wave. At the lower speed the pressure field produces the greater filtering velocity while the reverse is true at the higher speed. Since by eqn (10) the energy dissipated by the moving traction is proportional to square of this quantity, the relative energy dissipated by the two traction conditions appears to be speed dependent.

Finally, fluid stress at the lower surface of the layer is shown in Figs. 6 and 7. Consistent with analytical predictions, the indenter causes compressive stress in the fluid ahead and

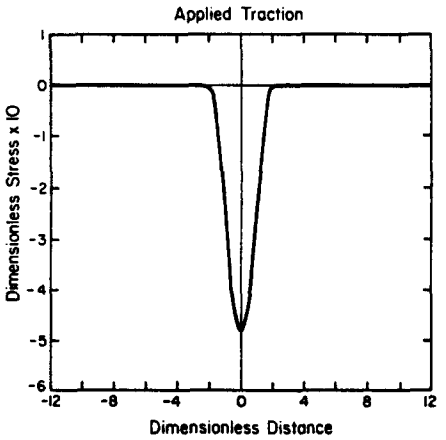

Fig. 1. Moving traction distribution.

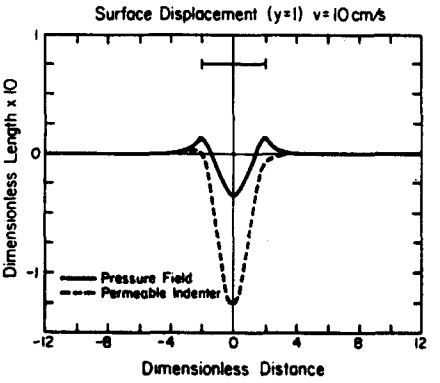

Fig. 2. Surface displacements; $v = 10$ cm/s.

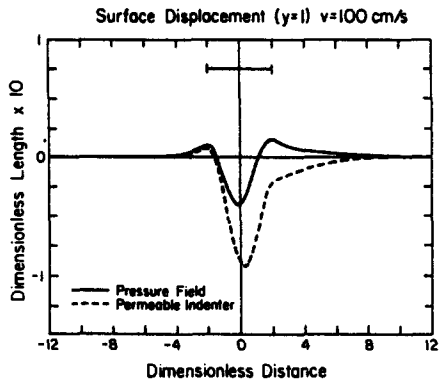

Fig. 3. Surface displacements; $v = 100$ cm/s.

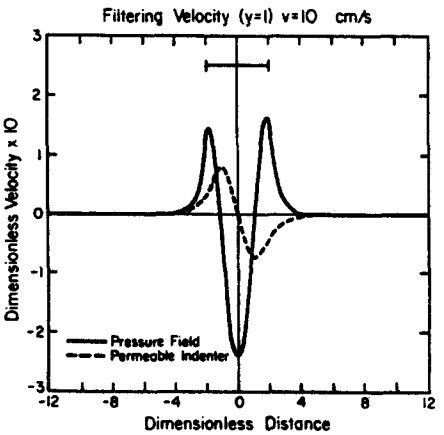

Fig. 4. Surface filtering velocity; $v = 10$ cm/s.

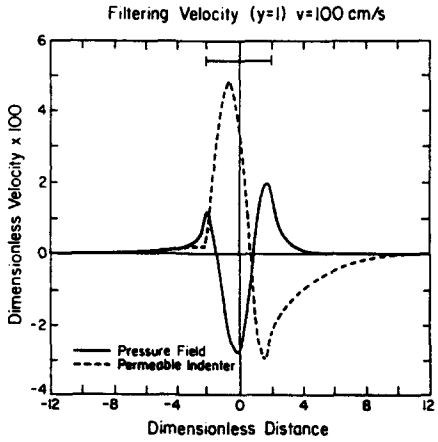

Fig. 5. Surface filtering velocity; $v = 100$ cm/s.

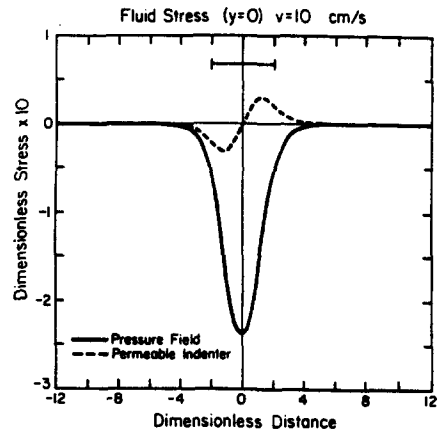

Fig. 6. Fluid stress at layer base; $v = 10$ cm/s.

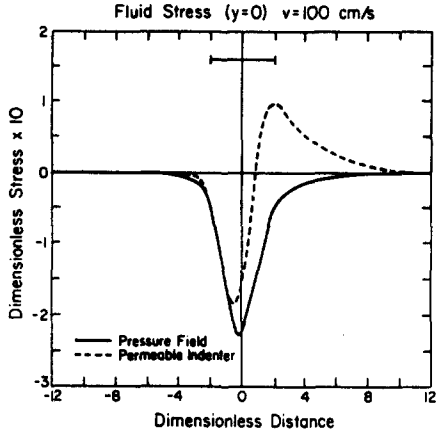

Fig. 7. Fluid stress at layer base; $v = 100$ cm/s.

relative tension (lower pressure) behind it while the reverse is true for the pressure wave. These effects are accentuated with increasing speed.

Because of the very different results for the response to the two types of surface tractions, it may be concluded that great care should be taken to accurately model the particular physical problem under investigation.

REFERENCES

1. A. K. Mukhopadyay and H. B. Kingsbury, A study of "Two dimensional flow in the press nip." *TAPPI J.* **63**, 63–90 (1980).
2. W. M. Lai and V. C. Mow, Flow field in a single layer model of articular cartilage created by a sliding load. 1979 *Adv. Bioengng, ASME* (1979).
3. T. Yamamoto, H. L. Koning, H. Sellmeijer and E. Van Hijum, On the response of a poro-elastic bed to water waves. *J. Fluid Mech.* **87**(1), 193–206 (1978).
4. M. A. Biot, General theory of three dimensional consolidation. *J. Appl. Phys.* **12**, 155–164 (1941).
5. M. A. Biot, Theory of elasticity and consolidation for a porous anisotropic solid. *J. Appl. Phys.* **26**, 182–185 (1955).
6. M. A. Biot, General solutions of the equations of elasticity and consolidation for a porous material. *J. Appl. Mech. (Trans ASME)* **23**, 91–96 (1956).
7. M. A. Biot, Theory of propagation of elastic waves in a fluid-saturated porous solid—I. Low-frequency range. *J. Acoust. Soc. Am.* **28**, 168–178 (1956).
8. M. A. Biot, Theory of propagation of elastic waves in a fluid saturated porous solid—II. Higher frequency range. *J. Acoust. Soc. Am.* **23**, 179-191 (1956).
9. M. A. Biot, Mechanics of deformation of acourstic propagation in porous media. *J. Appl. Phys.* **33**, 1482–1497 (1962).

10. J. E. Adkins, Nonlinear diffusion—I. Diffusion and flow of mixtures of fluids. *Philos. Trans. Royal Soc. Series A* **255**, 607–634 (1963).
11. J. E. Adkins, Nonlinear diffusion—II. Constitutive equations for mixtures of isotropic fluids. *Philo. Trans. Royal Soc. Series A* **255**, 635–654 (1963).
12. A. E. Green and J. E. Adkins, A contribution to the theory of nonlinear diffusion. *Arch. Rat. Mech. Anal.* **15**, 235 (1964).
13. A. E. Green and P. M. Naghdi, A dynamical theory of interacting continua. *Int. J. Engng Sci.* **3**, 231–248 (1965).
14. R. M. Bowen, Toward a thermodynamics and mechanics of mixtures. *Arch. Rat. Mech. Anal.* **24**, 370 (1967).
15. R. M. Bowen, Theory of mixtures. *Continuum Physics Vol. III Mixtures and EM Field Theories* (Edited by A. Cemal Erigen), pp. 560–569). Academic Press, New York (1976).
16. J. R. Rice and M. P. Clearly, Some basic stress diffusion solutions for fluid-saturated elastic porous media with compressible constitutents. *Rev. Geophysics and Space Physics* **14**, 227–241 (1976).
17. J. Bear, *Dynamics of Fluids in Porous Media*. Elsevier, New York (1972).
18. M. A. Biot and D. C. Willis, The elastic coefficients of the theory of consolidation. *J. Appl. Mech.* 594–601 (1957).
19. H. B. Kingsbury, Determination of material parameters of poroelastic media. *Proc. NATO Adv. Study Inst. on Mech. of Fluids in Porous Media* (1982), M. Nijhoff (to be published).
20. A. Verruijt, Elastic storage of aquiers. *Flow Through Porous Media* (Edited by Roger J. M. DeWiest), pp. 331–375. Academic Press, New York (1969).
21. A. Papoulis, *The Fourier Integral and its Applications*. McGraw Hill, New York (1962).
22. Y. K. Kim and H. B. Kingsbury, Dynamic characterization of poroelastic materials. *Experimental Mech.* **19**, 252–258 (1979).
23. M. Burke, On the response of poroelastic layers to moving loads. MMAE Thesis, Dept. Mechanical and Aerospace Engineering, University of Delaware, Newark, Delaware (1982).

APPENDIX A

Functions appearing in eqn (26)

$$H_{11}=\left[(Q_3+i)\left(R_1\frac{\omega}{\bar{k}^2-\omega^2}+\frac{R_5}{\omega}\right)+(i-Q_3)y\right]\sinh\omega y+\left[(Q_3+i)\left(R_1\frac{\omega}{\bar{k}^2-\omega^2}+y\right)+(i-Q_3)\frac{R_5}{\omega}\right]\cosh\omega y$$
$$+R_2R_6\left(\frac{\omega}{\omega^2-\bar{k}^2}\right)\frac{\omega}{\bar{k}}(1-iQ_3)\sinh\bar{k}y+R_6\left(\frac{\omega}{\omega^2-\bar{k}^2}\right)\left[R_2(1-iQ_3)+(1+iQ_3)R_3\left(\frac{\bar{k}^2-\omega^2}{\omega^2}\right)\right]\cosh\bar{k}y$$

$$H_{12}=Q_2\left[R_1\left(\frac{\omega}{\bar{k}^2-\omega^2}\right)+\frac{R_5}{\omega}-y\right]\sinh\omega y+\left[2+Q_2\left(R_1\left(\frac{\omega}{\bar{k}^2-\omega^2}\right)-\frac{R_5}{\omega}+y\right)\right]\cosh\omega y$$
$$-R_2R_6\left(\frac{\omega}{\omega^2-\bar{k}^2}\right)\frac{\omega}{\bar{k}}iQ_2\sinh\bar{k}y+R_6\frac{\omega}{\omega^2-\bar{k}^2}\left[iQ_2\left(R_3\frac{\bar{k}^2-\omega^2}{\omega^2}-R_2\right)-R_4\frac{\bar{k}^2-\omega^2}{\omega}\right]\cosh\bar{k}y$$

$$H_{21}=\left[(1-iQ_3)\left(R_1\frac{\omega}{\bar{k}^2-\omega^2}+y\right)\right]\sinh\omega y+\left[(1-iQ_3)R_1\frac{\omega}{\bar{k}^2-\omega^2}+(1+iQ_3)y\right]\cosh\omega y$$
$$+R_2R_7\left(\frac{\omega}{\omega^2-\bar{k}^2}\right)(1-iQ_3)\cosh\bar{k}y+R_7\left(\frac{\bar{k}}{\omega^2-\bar{k}^2}\right)\left[(1+iQ_3)R_3\frac{\bar{k}^2-\omega^2}{\omega^2}+(1-iQ_3)R_2\right]\sinh\bar{k}y$$

$$H_{22}=-\left[2i+iQ_2\left(R_1\frac{\omega}{\bar{k}^2-\omega^2}+y\right)\right]\sinh\omega y+iQ_2\left[y-R_1\frac{\omega}{\bar{k}^2-\omega^2}\right]\cosh\omega y-iQ_2R_2R_7\left(\frac{\omega}{\omega^2-\bar{k}^2}\right)\cosh\bar{k}y$$
$$+R_7\left(\frac{\bar{k}}{\omega^2-\bar{k}^2}\right)\left[iQ_2\left(R_3\frac{\bar{k}^2-\omega^2}{\omega^2}-R_2\right)-R_4\left(\frac{\bar{k}^2-\omega^2}{\omega}\right)\right]\sinh\bar{k}y$$

$$H_{31}=-2R_8(1-iQ_3)\sinh\omega y-2R_8(1+iQ_3)\cosh\omega y+R_2R_9\frac{\omega}{\bar{k}}(1-iQ_3)\sinh\bar{k}y$$
$$+R_9\left[R_2+R_3\frac{\bar{k}^2-\omega^2}{\omega^2}+iQ_3\left(R_3\frac{\bar{k}^2-\omega^2}{\omega^2}-R_2\right)\right]\cosh\bar{k}y$$

$$H_{32}=2R_8iQ_2\sinh\omega y-2R_8iQ_2\cosh\omega y-R_2R_9\frac{\omega}{\bar{k}}iQ_2\sinh\bar{k}y$$
$$+R_9\left[iQ_2\left(R_3\frac{\bar{k}^2-\omega^2}{\omega^2}-R_2\right)-R_4\left(\frac{\bar{k}^2-\omega^2}{\omega}\right)\right]\cosh\bar{k}y$$

$$G_{11}=\left[(Q_3+i)+\omega\left\{(Q_3+i)\left(R_1\frac{\omega}{\bar{k}^2-\omega^2}+\frac{R_5}{\omega}\right)+(i-Q_3)y\right\}\right]\cosh\omega y$$
$$+\left[(i-Q_3)+\omega\left\{(Q_3+i)\left(R_1\frac{\omega}{\bar{k}^2-\omega^2}+y\right)+(i-Q_3)\frac{R_5}{\omega}\right\}\right]\sinh\omega y$$
$$+R_2R_6\frac{\omega^2}{\omega^2-\bar{k}^2}(1-iQ_3)\cosh\bar{k}y+R_6\left(\frac{\omega\bar{k}}{\omega^2-\bar{k}^2}\right)\left[R_2(1-iQ_3)+(1+iQ_3)R_3\frac{\bar{k}^2-\omega^2}{\omega^2}\right]\sinh\bar{k}y$$

$$G_{12}=\left[Q_2+Q_2\omega\left\{R_1\frac{\omega}{\tilde{k}^2-\omega^2}+\frac{R_5}{\omega}-y\right\}\right]\cosh\omega y+\left[\omega\left\{2+Q_2\left(R_1\frac{\omega}{\tilde{k}^2-\omega^2}-\frac{R_5}{\omega}+y\right)\right\}-Q_2\right]\sinh\omega y$$
$$-R_2R_6\left(\frac{\omega^2}{\omega^2-\tilde{k}^2}\right)iQ_2\cosh\tilde{k}y+R_6\frac{\omega\tilde{k}}{\omega^2-\tilde{k}^2}\left[iQ_2\left(R_3\frac{\tilde{k}^2-\omega^2}{\omega^2}-R_2\right)-R_4\frac{\tilde{k}^2-\omega^2}{\omega}\right]\sinh\tilde{k}y$$

$$G_{21}=\left[\omega\left\{(1-iQ_3)\left(R_1\frac{\omega}{\tilde{k}^2-\omega^2}+y\right)\right\}+(1+iQ_3)\right]\cosh\omega y$$
$$+\left[\omega\left\{(1-iQ_3)R_1\frac{\omega}{\tilde{k}^2-\omega^2}+(1+iQ_3)y\right\}+(1-iQ_3)\right]\sinh\omega y+R_7\left(\frac{\tilde{k}^2}{\omega^2-\tilde{k}^2}\right)\left[(1+iQ_3)R_3\frac{\tilde{k}^2-\omega^2}{\omega^2}\right.$$
$$\left.+(1-iQ_3)R_2\right]\cosh\tilde{k}y$$

$$G_{22}=\left[iQ_2-\omega\left\{2i+iQ_2\left(R_1\frac{\omega}{\tilde{k}^2-\omega^2}+y\right)\right\}\right]\cosh\omega y+\left[\omega iQ_2\left(y-R_1\frac{\omega}{\tilde{k}^2-\omega^2}\right)-iQ_2\right]\sinh\omega y$$
$$-iQ_2R_2R_7\left(\frac{\omega\tilde{k}}{\omega^2-\tilde{k}^2}\right)\sinh\tilde{k}y+R_7\left(\frac{\tilde{k}^2}{\omega^2-\tilde{k}^2}\right)\left[iQ_2\left(R_3\frac{\tilde{k}^2-\omega^2}{\omega^2}-R_2\right)-R_4\left(\frac{\tilde{k}^2-\omega^2}{\omega}\right)\right]\cosh\tilde{k}y$$

$$G_{31}=-2R_8(1-iQ_3)\omega\cosh\omega y-2R_8(1+iQ_3)\omega\sinh\omega y+R_2R_9\omega(1-iQ_3)\cosh\tilde{k}y$$
$$+R_9R_2+R_3\frac{\tilde{k}^2-\omega^2}{\omega^2}+iQ_3\left(R_3\frac{\tilde{k}^2-\omega^2}{\omega^2}-R_2\right)\tilde{k}\sinh\tilde{k}y$$

$$G_{32}=2R_8iQ_2\omega\cosh\omega y-2R_8iQ_2\omega\sinh\omega y-R_2R_9\omega iQ_2\cosh\tilde{k}y$$
$$+R_9\left[iQ_2\left(R_3\frac{\tilde{k}^2-\omega^2}{\omega^2}-R_2\right)-R_4\left(\frac{\tilde{k}^2-\omega^2}{\omega}\right)k\sinh\tilde{k}y\right.$$

where

$$R_1=\frac{2\alpha/fB/A}{1+A-\alpha/fB}\qquad R_7=-iR_6$$
$$R_2=\frac{(1+A)}{B}R_1\qquad R_8=\alpha/fB/A$$
$$R_3=\frac{(A+2)(A+1)}{AB}\qquad R_9=B-\alpha/f\frac{B^2}{(1+A)}$$
$$R_4=i2\frac{(1+A)}{B}\qquad R_{10}=\alpha/f\frac{(\lambda-\gamma^2/\beta)}{\mu}$$
$$R_5=\frac{(A+2)}{A}\qquad R_{11}=\alpha/f\frac{(\lambda-\gamma^2/\beta+2\mu)}{\mu}$$
$$R_6=i\frac{B}{1+A}\qquad R_{12}=\gamma/\beta$$

$$Q_1=\sinh\tilde{k}[iR_7\tilde{k}/c(ic/\omega R_3-R_2)]$$
$$-\cosh\tilde{k}[R_2R_7i\omega/c]-\sinh\omega\left[\omega(1-iR_{1/c})-\frac{(1+R_5)}{2}+\cosh\omega\left[\omega(1+iR_{1/c})-\frac{(1+R_5)}{2}\right]\right.$$

$$Q_2=1/Q_1\{2\omega\sinh\omega+R_4R_6\tilde{k}\sinh\tilde{k}\}$$

$$Q_3=\frac{1}{Q_1}\left\{\left[\omega(i+R_{1/c})+i\frac{(1+R_5)}{2}\right][\cosh\omega+\sinh\omega]+\sinh\tilde{k}[iR_6\tilde{k}/c(R_2+ic/\omega R_3)]\right.$$
$$\left.+\cosh\tilde{k}[i\omega/cR_2R_6]\right\}.$$

Pressure field

$$B_3=\left(\frac{-\hat{P}_s}{\Delta}\right)\{f(i\omega R_{10}H_{12}+R_{11}G_{22})-[(1-f)-fR_{12}]H_{32}\}|_{y=1}$$

$$B_2=\left(\frac{-\hat{P}_s}{\Delta}\right)\{H_{31}[(1-f)-fR_{12}]-f(i\omega R_{10}H_{11}+R_{11}G_{21})\}|_{y=1}$$

$$\Delta=[H_{31}(i\omega R_{10}H_{12}+R_{11}G_{22})-H_{32}(i\omega R_{10}H_{11}+R_{11}G_{21})]|_{y=1}.$$

Indenter

$$B_3 = -\left[\frac{H_{32}}{H_{31}}\right]_{\gamma=1} B_2$$

$$B_2 = \left[\frac{-1}{R_{10}i\omega\left(H_{12} - \dfrac{H_{11}H_{32}}{H_{31}}\right) + R_{11}\left(G_{22} - \dfrac{H_{32}G_{21}}{H_{31}}\right)}\right]_{\gamma=1} P_s.$$

APPENDIX B

Poroelastic material constants of wool felt-water (Ref. [22])

$\lambda = 7.9 \times 10^5$ Pa $\quad f = 0.7$
$\mu = 5.3 \times 10^5$ Pa $\quad \alpha = 0.9$
$\beta = 4.0 \times 10^6$ Pa $\quad K = 3.7 \times 10^{-9}$ cm^2
$\sigma = 1.2 \times 10^6$ Pa $\quad \eta = 0.89 \times 110^{-3}$ Pa-sec.